Fourier Transform InfraRed spectroscopy contribution to disentangle nanomaterial (DWCNT, TiO 2) impacts on tomato plants

Clarisse Liné, Juan Reyes-Herrera, Mansi Bakshi, Mohammad Wazne, Valentin Costa, David Roujol, Elisabeth Jamet, Hiram Castillo-Michel, Emmanuel Flahaut, Camille Larue

Fourier Transform InfraRed spectroscopy contribution to disentangle nanomaterial (DWCNT, TiO_2) impacts on tomato plants

Clarisse Liné[a,b], Juan Reyes-Herrera[c], Mansi Bakshi [a,d], Mohammad Wazne[c], Valentin Costa[a], David Roujol[e], Elisabeth Jamet[e], Hiram Castillo-Michel[c], Emmanuel Flahaut[b] and Camille Larue[a*]

[a]Laboratoire Ecologie Fonctionnelle et Environnement, Université de Toulouse, CNRS, Toulouse, France
[b] CIRIMAT, Université de Toulouse, CNRS, INPT, UPS, UMR CNRS-UPS-INP N°5085, Université Toulouse 3 Paul Sabatier, Bât. CIRIMAT, 118, route de Narbonne, 31062 Toulouse cedex 9, France
[c]Beamline ID21, European Synchrotron Radiation Facility (ESRF), Grenoble, France
[d]Institute of Environment and Sustainable Development, Banaras Hindu University, Varanasi, India
[e]Laboratoire de Recherche en Sciences Végétales, Université de Toulouse, CNRS, UPS, Auzeville-Tolosane, France

Abstract. Carbon nanotubes (CNTs) and titanium dioxide nanoparticles (TiO_2-NPs) are among the most used nanomaterials (NMs). However, their impacts especially on the terrestrial ecosystems and on plants are still controversial. Apart from obvious physico-chemical differences, a possible explanation of these contrasting results could be the wide range of methods used to evaluate the toxicity at different levels of plant physiology. Fourier Transformed InfraRed (FTIR) spectroscopy is a sensitive and widely informative technique that probes the chemical composition of plants. In this study, we investigated the impacts of CNTs and TiO_2-NPs (100 and 500 $mg.kg^{-1}$) on tomato plants after 5, 10, 15 and 20 days of exposure in soil. Using morphological parameters, no toxicity was found except after 15 days of exposure (-57% in height and -62% in foliar area for plants exposed to 100 $mg.kg^{-1}$ TiO_2-NPs, but no impact after CNT exposure) while FTIR revealed effects of the two NMs starting after 5 days of exposure and being maximum after 15 days. After spectral data treatment optimization, FTIR results suggested modifications in leaf cell wall components of plants subjected to both NMs. Microarray polymer profiling confirmed changes in xyloglucan and homogalacturonan levels for plants exposed to TiO_2-NPs. In summary, FTIR was an effective screening method to evaluate the impacts of NMs on tomato plants and to identify their implications on the plant cell walls.

1. Introduction

Over the last two decades, nanotechnologies have become increasingly important. Indeed, nanomaterials (NMs) present unique properties such as a large specific surface area which can be useful in many domains such as electronics, materials or food industry[1]. In 2020, the Dutch Nanodatabase revealed that a total of 5000 consumer products officially contained NMs[2]. Investigations about their possible use in medicine[3] or in agriculture[4] are also in progress.

Carbon nanotubes (CNTs) and titanium dioxide nanoparticles (TiO_2-NPs) are among the most widely used NMs[2]. CNTs are part of the carbon-based NM family. They have remarkable optical, electrical, thermal, mechanical and chemical properties[5] and are mainly used in batteries, plastic additives or sporting goods[6]. TiO_2-NPs are well known for photocatalytic applications[7] and are included for example in food additives[8] or cosmetics[9]. Since NM applications are steadily increasing, their release in the environment, intentionally or not, is of great concern.

Assessing NM concentrations in the environment is a major bottleneck in ecotoxicology. Modeling studies were carried out on some NMs to evaluate this information in different environmental compartments. TiO_2-NPs have been identified as one of the most concerning NMs due to the high concentrations forecast: around 61 $mg.kg^{-1}$ in sludge treated soils against 12 $\mu g.kg^{-1}$ for CNTs[10].

NM impacts on terrestrial ecosystems are still controversial, in particular on plants[11]. Indeed, some authors reported higher germination rate and better yield after exposure to CNTs while other studies highlighted decreased root length or oxidative stress[11]. The same conclusions were reached for TiO_2-NP impacts on plants[12]: while some beneficial effects were reported such as a higher germination rate or increased root and shoot length[13–16], other works described decreased germination rate, plant growth or genotoxic effects[17–19]. Until now, the specific mechanisms implied in NM uptake (active *vs.* passive, apoplast *vs.*

symplast, among other questions) and impact (*e.g.* nano specific or ion related, oxidative stress mediated) are still to be identified and require further research[20].

Apart from obvious physico-chemical differences, a possible explanation of these contrasting phytotoxicity results may also be the method used to evaluate NM impacts on plants. Many biomarkers can be assessed from the morphological to the gene scale showing variable sensitivity. Their use to evaluate plant health is conclusive when many of them are combined. But in the literature, most of the studies use a limited number of biomarkers leading to a potentially partial image of the toxicity effects and thus a biased risk assessment. The availability of routine, standardized and widely informative analytical methods to evaluate NM toxicity is a key to fill this current gap of knowledge[21].

Fourier Transform InfraRed (FTIR) spectroscopy is a technique based on the vibrational state of molecules. It allows the acquisition of a spectrum combining information on a multitude of compounds, unlike chemical dosages which give access only to one compound (*e.g.* specific enzyme or secondary metabolite) after a series of reactions[22]. There are two types of acquisition modes: either bulk analysis of the whole plant (few minutes per sample) or 2D-imaging mode of cross sections (few hours per map)[23]. In bulk mode, sample preparation is very simple, consisting of grinding dry materials thus reducing artifacts. Therefore, FTIR is a widely informative, easy to set-up and fast technique that could be used to screen NM effects on different organisms. In plant biology, FTIR has been mainly used to characterize plant cell wall components in a highly sensitive and more time-efficient manner than traditional methods which require isolation, extraction and fractionation of the different cell wall components[24–28]. Recently, FTIR has been used in ecotoxicological studies to analyze changes occurring in biological materials after exposure to biotic or abiotic stresses[23,29–36]. For instance, Morales *et al*., Servin et *al*. and Zhao *et al*. highlighted changes in the chemical environment of carbohydrates of both cilantro and cucumber exposed to CeO_2, ZnO or TiO_2 NPs[33,35,36]. Radish sprouts exposed to Ag-NPs also exhibited modifications of their IR spectral signature in the region related to lipids, proteins and particularly structural component peaks such as lignin, pectin and

cellulose[34]. Likewise, very recently, we applied FTIR to evaluate the influence of plant species on their response to a CNT contamination highlighting the role of cell wall composition[32]. Indeed, it has been demonstrated several times that cell walls play a crucial role in plant response to abiotic stresses[37]. Plant cell walls are composed of complex polysaccharides and a small amount of proteins and their composition can be modified in response to stress[37–40].

However, FTIR data processing is tedious due to spectrum complexity. Indeed, it contains overlapping signals coming from many molecular bonds. A purely visual inspection of spectra is often insufficient to draw a conclusion. Several factors could weaken this analysis and its subsequent conclusions: i) sometimes, minor spectral differences not detected with the bare eye may contain critical information, ii) the baseline may vary from one sample to another, iii) instrumental noise could induce bias. For these reasons, it is important to find a way to process and analyze the data in a more systematic way using statistical approaches (*i.e.* supervised classification, clustering method) in order to obtain meaningful information [41].

The main goal of this study was to develop the FTIR approach to evaluate the comparative impacts of two types of NMs (CNTs and TiO_2-NPs) taking into account: (i) different NM concentrations and (ii) different exposure durations. Seedlings of tomato (*Solanum lycopersicum* L.) were grown in soil contaminated with CNTs or TiO_2-NPs at two different concentrations (100 and 500 $mg.kg^{-1}$ of soil) during different durations (5, 10, 15 and 20 days). FTIR was used as the main technique to evaluate the impact of the two NMs on tomato plants. Complementary morphological biomarkers were also assessed (height, biomass, number of leaves, leaf surface area). Finally, to better understand the FTIR data, the cell wall composition was further analyzed by microarray polymer profiling. Developing a reliable technique to assess in a screening mode the biological effects of many different types of NMs is mandatory to accelerate the risk assessment of these new materials being disseminated or intentionally introduced in our environment on a daily basis.

2. Materials and methods

2.1. Nanomaterials

TiO_2-NPs (ref 718467, Aeroxide P25, Sigma-Aldrich, Merck KGaA, Darmstadt, Germany) were characterized in a previous experiment (same batch) and were composed of 80% anatase and 20% rutile with a nominal diameter of 25.0 ± 5.7 nm[19]. They had a specific surface area of 46 ± 1 $m^2.g^{-1}$ (Figure S1A)[19].

Double walled CNTs were synthesized by catalytic chemical vapor deposition (CCVD) at 1000°C of a mixture of CH_4 (18 mol.%) and H_2 using a Co:Mo/MgO-based catalyst (chemical composition: $Mg_{0.99}Co_{0.0075}MgO_{0.0025}$)[42]. The outer diameter ranged from 1 to 3 nm and the length varied from 1 to 100 microns (Figure S1B)[42]. The specific surface area was 980 $m^2.g^{-1}$ (Brunauer, Emmett and Teller (BET) method; Micromerics Flow Sorb II 2300, Micromeritics, Norcross, GA, USA).

Fresh NM suspension at 1 $g.L^{-1}$ were prepared with ultrapure water directly before use and dispersed using a sonication bath for 10 min (Elmasonic S30H, 280 W, Elma, Singen, Germany).

2.2. Soil characteristics and contamination

A silty sand soil (according to the United State Department of Agriculture[43]) was used for this experiment (Lufa-Speyer, 2.1, Speyer, Germany) with a composition of 88.0% sand, 9.1% silt and 2.9% clay. It contained 0.71 ± 0.08 % organic carbon, 0.06 ± 0.01 % nitrogen, had a pH of 4.9 ± 0.3 and a cation exchange capacity of 4.3 ± 0.6 meq/100 g of soil. The soil water capacity was 60 mL/100 g of soil.

CNT or TiO_2-NP suspensions were added to the dry soil to reach a concentration of 100 or 500 mg NMs/kg dry soil (ratio liquid/soil = 1/1 in mass). After 2 h on a shaker table, the soil mixture was filtered to remove the water in excess. This soil preparation protocol ensured a soil contamination as homogeneous as possible. These concentrations were chosen to be relevant for TiO_2-NP contamination in sludge amended soils[10] and comparable between NMs.

2.3. Plant material and cultivation

Organic seeds of tomato *Solanum lycopersicum* L. (var. Red Robin) were obtained from the French seed company Germinance (Soucelles, France) and surface-sterilized using $Ca(ClO)_2$ (1%). Seedlings were first grown in hydroponic conditions for 3 weeks until they reached the 5 leaf-stage. Plants were then placed into control or contaminated soil until harvest after 5, 10, 15 or 20 days of exposure. Exposure durations were chosen based on a literature study showing that more than 65% of articles studying CNT impacts on plants used exposure duration of less than 15 days[11]. Each exposure duration corresponded to an independent experiment. The experiments were performed in a growth chamber with controlled parameters: 10 h light/14 h dark photoperiod; 24°C during the day and 22°C during the night; and a hygrometry of 85%.

Five different exposure conditions were set-up: control (only soil without NM contamination), 100 mg CNTs/kg dry soil (CNT 100), 500 mg CNT/kg dry soil (CNT 500), 100 mg TiO_2-NPs/kg dry soil (TiO_2 100) and 500 mg TiO_2-NPs/kg dry soil (TiO_2 500). Five biological replicates were performed in each case.

Morphological parameters were monitored every day (plant height and number of leaves). Upon harvest, other morphological parameters were measured (total fresh leaf biomass and foliar surface area using a camera and ImageJ software[44]). Leaves were dried at 50°C during 24 h prior to FTIR analysis.

2.4. FTIR analysis

About 20 mg dry leaves were ground 2 x 15 s at maximum speed using a FastPrep grinding machine (MP Biomedicals, Illkirch-Graffenstaden, France). Each powdered sample was analyzed in attenuated total reflectance (ATR) mode using a diamond crystal (Thermo Nicolet Nexus, Smart Orbit, Thermo Fisher Scientific, Waltham, USA). Infrared spectra were collected in the range 4000 - 400 cm^{-1}. All the samples (5

biological replicates) were analyzed in (technical) triplicates and each spectrum was the sum of 64 scans. OMNIC software (Thermo Fischer Scientific©) was used to export spectra.

2.5. Chemometric analysis for FTIR data

A chemometric analysis of FTIR spectra was developed using Orange software (BioLab, Ljubljana, Slovenia)[45] including the add-on Spectroscopy[46]. During the first step, data were pre-processed to eliminate possible analytical biases (such as detector noise and atmospheric background)[23]. For this, a Savitzky-Golay filter was applied (point window: 21, polynomial order: 2, derivative order: 2). This filter is based on simplified least square procedures and permits removal of various instrumental and scattering effects. A vector normalization was then applied to minimize the effects of the source power fluctuations as well as to overcome variations due to the amount of leaf powder analyzed. The last step of the pre-processing was to select the region of interest in order to avoid background interferences[23,47]. Here, we focused on two regions of the spectra: between 2900 and 2700 cm^{-1} corresponding to the lipid region and between 1800 and 800 cm^{-1} corresponding to the so-called fingerprint region (including proteins and polysaccharides). The region between 1800 and 2700 cm^{-1} was removed because it mainly corresponded to background interferences. With this pre-process, the robustness and accuracy of subsequent analyses were improved and the interpretability of the data was increased by correcting issues associated with spectral data acquisition.

A multivariate analysis was then performed on the pre-processed spectra with first a principal component analysis (PCA), followed by a linear discriminant analysis (LDA) when necessary[41]. PCA is an unsupervised method which searches for directions where data have the largest variance, whose results can show data structural information. While, LDA is a supervised method that looks for projections that maximize the ratio between-class to within-class. The combination of both methods is particularly useful when the

number of variables is large, especially if the number of observations (samples) is lower than the number of variables (wavenumbers) as in this work. PCA allows reducing the number of variables, in this analysis from 1246 variables to 10 components, the reduced dataset being then analyzed by LDA to enhance differences between the classes, if any.

In order to identify the wavenumbers contributing the most to differences among groups, a logistic regression was run on the pre-processed spectra. The logistic regression is a predictive model that yields the probability of occurrence of an event by fitting data to a logistic curve. The least absolute shrinkage and selection operator (LASSO) method was used to perform the regularization and feature selection. Most relevant wavenumbers were identified by obtaining logistic regression coefficients; this feature extraction method has been already used in ATR-FTIR data analysis[48]. For testing the robustness of the statistical model used, the area under a receiver operating characteristics (ROC) curve (AUC) and K-fold cross validation were used[41]. Finally, to compare the different spectra among them, the area under differing absorption peaks was calculated by integrating the area starting from 0 on the pre-processed spectra.

2.6. Cell wall composition by polysaccharide microarray analysis

The cell wall composition was assessed according to Moller et al.[49]. This technique integrates the sequential extraction of polysaccharides from cell walls, followed by generation of microarrays, which are probed with monoclonal antibodies (mAbs) with specificities for cell wall epitopes.

Cell wall polysaccharides were sequentially extracted from homogenates using three solvents: (i) 50 mM diamino-cyclo-hexane-tetra-acetic acid (CDTA), pH 7.5, (ii) 4 M NaOH with 1% v/v $NaBH_4$, and (iii) cadoxen (31% v/v 1,2-diaminoethane with 0.78 M CdO). The three extraction solvents used are known to solubilize pectins, non-cellulosic polysaccharides, and cellulose, respectively. For each extraction, a ratio of 6 µL

solvent for 1 mg fresh biomass was added to each tube before incubation with shaking for 1 h. After centrifugation at 2500 *g* for 10 min, the supernatants were removed prior to addition of the next solvent to pellets. All the supernatants were finally stored at 4°C. Forty µL of diluted extracts (2/50, vol/vol) in TBS (Tris-HCl 20 mM pH 7.5, NaCl 150 mM, pH 7.0) were then loaded in each well of a Bio-Dot apparatus (BIO-RAD, Marnes-la-Coquette, France) onto nitrocellulose membranes (Sigma-Aldrich). After blocking TBS-T/BSA 0.05% (0.05% Tween), the arrays were probed overnight at 4°C with primary mAbs directed against different cell wall epitopes (https://plantcellwalls.leeds.ac.uk/plantprobes/) at a 1/250 dilution (vol/vol) in TBS-T/BSA 0.05%: LM19 (for non-methylated homogalacturonans, HG), LM20 (for methylated HG, mHG), LM25 for the XLLG, XXLG and XXXG motifs of xyloglucans, XG), LM15 (for the XXXG motif of XG and to some extent single galactosyl substitution of the XXXG oligosaccharide, and LM24 (for the XLLG motif of XG). After washing in TBS-T, the arrays were probed with anti-rat IgG secondary antibodies conjugated to alkaline phosphatase (Sigma-Aldrich) at a 1/10,000 dilution (vol/vol) for 2 h before washing and developing in a BCIP/NBT (5-bromo-4-chloro-3¢-indolyphosphate/nitro-blue tetrazolium chloride) substrate. To check the activity of the mAbs, commercially purified polysaccharides were used as positive controls: polygalacturonic acid (HG, Sigma-Aldrich), polygalacturonic acid methyl ester (mHG, Sigma-Aldrich), and XG (Megazyme, Libios, Pontcharra-sur-Turdine, France). The arrays were scanned using an Epson Perfection V370 Photo (Nagano, Japon). Color intensity of each spot was quantified thanks to ImageJ software.

2.7. Statistical analysis

Data (morphological parameters) were checked for homoscedasticity and normality. When assumptions were met for parametric analyses, a two-way ANOVA was used. Otherwise, a Kruskal-Wallis test was applied. A PCA was also performed on the full dataset. All statistical analyses were carried out using the

213 RStudio statistical software[50] (version 1.1.453) with multcompView[51], lsmeans[52], pgirmess[53], ggplot2[54]
214 packages.

215

216 **3. Results**

217 **3.1. Morphological responses**

218 Plant height and number of leaves were recorded during the time course of the four experiments (5, 10,
219 15 and 20 days of exposure) as well as plant biomass and leaf area at the end of the experiments. These
220 data are available in the Supplementary files (Figure S2, S3). No significant impact of NM exposure after 5,
221 10 and 20 days was evidenced for these parameters.

222 Differences were only detected after 15 days of exposure. Indeed, plants exposed to 100 mg.kg^{-1} TiO_2-NPs
223 were significantly smaller than the control (-57%, p-value < 0.05, Figure 1A). Plants exposed to 500 mg.kg^{-}
224 ^{1} TiO_2-NPs were 28% smaller than the control plant but this decrease was not significantly different (2.3 ±
225 0.3 cm for the control and 1.6 ± 0.4 cm for 500 mg.kg^{-1} TiO_2-NPs). Although plants exposed to both CNT
226 concentrations for 15 days were not significantly different in height from the control plants, there was an
227 increase of 26% and 28% in soils contaminated with 100 and 500 mg.kg-^{1} CNT, respectively (2.3 ± 0.3 cm
228 for control, 2.9 ± 0.8 cm for 100 mg.kg^{-1} CNT and 2.9 ± 0.5 cm for 500 mg.kg^{-1} CNT).

229 The number of additional leaves at the end of the treatments was not significantly different between
230 conditions (Figure S2B); plants displayed an average of 1.8 additional leaf after 15 days.

231 On the one hand, the total leaf area of plants exposed to the two TiO_2-NP concentrations was decreased
232 after 15 days of exposure: 7.2 ± 2.4 cm² for 100 mg.kg^{-1} TiO_2-NPs and 8.9 ± 2.6 cm² for 500 mg.kg^{-1} TiO_2-
233 NPs while that of the control was at 19.0 ± 2.7 cm² (p-value < 0.001, Figure 1B). On the other hand, no
234 significant difference was found for plants exposed to CNTs.

Plant biomass was not significantly different for treated plants compared to the control after 15 days of exposure but different in between exposed plants (p-value < 0.001, Figure 1C). However, plants exposed to 500 mg.kg^{-1} CNTs exhibited a trend for higher biomass compared to the control (+30%) while plants exposed to 100 mg.kg^{-1} TiO_2-NPs tended to be lighter than the control (-64%).

The PCA analysis of the different morphological parameters highlighted a significant impact of TiO_2-NPs on tomato morphology after 15 days of exposure with a decrease in most of the assessed parameters while CNTs had a more mitigated impact at this developmental level (Figure 1D).

3.2. Leaf chemical composition after FTIR analysis

Again the highest differences were visible after 15 days of treatment, even though NM impact was visible already after 5 days, opposite to what was observed from morphological parameters. PC-LDA analyses on FTIR data for 5, 10 and 20 days of NM exposure are available in supplementary data (Figure S4).

After the different contaminant exposure, the composition of leaves was significantly different between the three treatments according to the PC-LDA (Figure 2A). Looking at the distance of the barycenter of the ellipses, the plants exposed to 500 mg.kg^{-1} CNT exhibited the highest differences in comparison to the control while those exposed to 100 mg.kg^{-1} CNT showed the lowest differences. Both groups of the TiO_2-NP conditions were almost at the same distance from the control, but in the opposite direction to CNT groups along the component 1 axis. This result suggests that the leaf composition is different between plants exposed to CNTs and TiO_2-NPs, confirming the different impacts seen at the morphological level (decreased growth after TiO_2-NP exposure *vs*. trend for an increase after CNT exposure).

Once a significant cluster structure was identified for the 15 day treatment case, feature extraction was performed with a logistic regression model. This model was tested by a stratified 3-fold cross-validation

method, obtaining average over classes scores of 0.932 of AUC, 0.889 of precision and a recall of 0.852, notice that a strong and robust model have scores close to one[41]. A difference was highlighted in the so-called "lipid region" (Figure 2B, peak A, Table 1) with higher relative amounts for plants exposed to the four different treatments in comparison to the control with the highest amount in leaves of plants grown on soil contaminated by CNTs at 500 $mg.kg^{-1}$ (+ 29 ± 2.3% of the area under the peak for CNT 500 in comparison to the control). In the amide II peak[55,56], leaves of plants grown on contaminated soils exhibited an increase in peak area in comparison to the control except for CNT 500 (12 ± 1% increase for CNT 100, 6 ± 7 % for TiO_2 100 and 6 ± 1% TiO_2 500) (Figure 2B, peak B; Table 1). Polysaccharides[38,47,56,57] also seemed to be impacted with differences in the areas of peaks C (1320 - 1312 cm^{-1}) and D (1160 - 1155 cm^{-1}). Exposed plants displayed an increase in peak C area while a slight decrease in the peak D area was observed. Between 1080 and 1070 cm^{-1} corresponding to hemicellulose[38,47,56] (Figure 2B, peak E; Table 1), a slight decrease in the peak area was detected for the leaves of plants grown on all contaminated soils. Finally, a decrease in areas of peak F corresponding to pectin and various polysaccharides[47,56,57] (1052 – 990 cm^{-1}, Figure 2B, peak F; Table 1) was noticed for the plants grown in soil contaminated with CNTs whereas an increase in peak F area was detected for the plants grown with TiO_2-NPs. Altogether, most of the differences observed between the FTIR spectra were related to cell wall components (pectin, cellulose or hemicellulose).

The signals obtained here were averaged on the whole leaf biomass. For further analysis, chemical composition of the leaves was observed considering their age on the two 500 $mg.kg^{-1}$ NM treatments (Figure 3). Overall, the oldest and the youngest (at early development stage during contaminant exposure) leaves were the least impacted by NM contamination; leaves of plants exposed to TiO_2-NPs, in particular, had a chemical composition very similar to those of control plants (Figure 3A,D). However, intermediate leaves (Figure 3B, C) exposed to NM displayed different FTIR signatures than control plants, but similar in-between them according to the PC-LDA with overlapping ellipses for both CNT and TiO_2-NP treated leaves.

3.3. Cell wall composition by polysaccharide microarray analysis

As FTIR analyses suggested a strong impact of NM treatments on cell wall components, a more precise characterization was carried out on three cell wall fractions enriched in pectin, hemicellulose or cellulose. Several mAbs recognizing the main polysaccharides found in dicot cell walls were used, namely HG, mHG and different XG epitopes. No significant signal was obtained with LM20 (recognition of mHG), and LM24 (recognition of XLLG motifs of XG) mAbs (results not shown). Signals were observed with the three other mAbs: LM19 (recognition of HG), LM25 and LM15 (recognition of XLLG, XXLG and XXXG motifs and of XXXG motifs of XG, respectively) (Figure 4).

Significant differences were found for HG (LM19) in the pectin-enriched fraction of leaves of plants exposed for 15 days to 500 $mg.kg^{-1}$ TiO_2-NPs with a 58% increase ($p= 0.028$). The LM19 signal also increased by nearly two-fold in the hemicellulose-enriched fraction although this increase was not significant. Significant differences were also detected with LM25 for the same condition (500 $mg.kg^{-1}$ TiO_2-NPs) in the hemicellulose-enriched fraction (+37% in comparison to the control, $p= 0.046$). However, no significant difference was found with LM15 specific for the XXXG motif of XG. It can be concluded that XXLG is the only XG motif whose amount was modified in leaves when plants were exposed to 500 $mg.kg^{-1}$ TiO_2-NPs for 15 days. For CNT, no significant difference was found with all the mAbs tested here.

Altogether, it was not possible to detect mHG (LM19) or the XLLG motif of XG (LM24) in the tomato leaves whatever the treatment. Significant changes were only observed after the treatment with 500 $mg.kg^{-1}$ TiO_2-NPs, corresponding to an increase in the amount of HG (LM19) and of the XXLG motif of XG (LM25, vs LM15 and LM24).

4. Discussion

In this study, **FTIR** spectroscopy appeared to be a more sensitive technique to detect the impact of NM treatment on plant compared to the traditionally used morphological biomarkers. Indeed, FTIR analysis revealed a plant response to NM contamination even at the shortest time of exposure (5 days). Looking at the morphological parameters, few differences were visible only after 15 days but not earlier which seemed to be compensated later. FTIR also allowed assessing NM impacts on several biomacromolecules (*i.e.* lipids, polysaccharides) in one single analysis, thus permitting to dedicate further research efforts to look at the modifications of cell wall composition under the influence of NM exposure. The developed chemometric analysis was quite powerful in highlighting differences between the experimental conditions in an automated way, which would have not been possible by visual inspection of the FTIR spectra. FTIR spectroscopy is thus a relevant method to identify early impacts of NMs on plants in a fast and reliable way, thereby permitting a screening approach.

In this soil experiment, plant response to NMs was not **dose-dependent** since most of the time, impacts were not higher at the highest concentration. One hypothesis possibly explaining this result is that NMs can have different behaviors in the environment depending on the concentration used. Indeed, when the concentration is increased, it also leads to more chances for hetero- and homo-agglomeration phenomena which would result in decreasing NM mobility and bioavailability in soils[58,59].

The impacts of both NMs tended to increase with **time** until 15 days of exposure, and then decreased (20 days: no detectable difference in morphological biomarkers and lower impact on biomacromolecules such as lipids, polysaccharides or proteins as demonstrated by FTIR analysis). This decrease in impacts after 15 days of exposure could suggest a plant recovery. Likewise, when studying NM impact on individual leaves of different ages, the oldest one (*i.e.* exposed for the longest period) was the least impacted in its chemical composition while clear differences were visible on other fully-expanded leaves. This could also correspond to a recovery or adaptation at the leaf level. Very little has been done so far to study plant recovery after a NM exposure. One study reported that TiO_2-NPs had no major impact on tomato plants

upon harvest (after 5 months of exposure), but some markers indicated that plants might have gone through oxidative stress earlier in their life cycle[29]. It has also been shown after exposure to different heavy metals (Zn, Co, Cd, Ni, Mn) that the detoxification response was triggered during the first days of exposure and then decreased back nearly to its basal level after 9 days[60]. It would thus be interesting to investigate NM impacts on biomacromolecules under chronic exposure conditions to confirm this hypothesis and further improve risk assessment strategies.

CNTs and TiO_2-NPs have been chosen here as they are two very different NMs; in particular, they vary in shape (tubular for CNTs *vs.* spherical for TiO_2-NPs), in surface chemistry (carbon *vs*. metal oxide), in diameter (1-3 nm diameter for CNTs *vs.* 25 nm for TiO_2-NPs) but they are both very insoluble. Their behavior and impacts are thus expected to be quite different. Indeed, at the morphological level, TiO_2-NPs inhibited tomato development while CNTs tended to stimulate it. These results are consistent with previously published literature[19,61]. However, regarding biomacromolecule composition NM triggered quite similar impacts, especially on cell wall components, which might suggest a common response of plants upon exposure to CNTs or TiO_2-NPs.

FTIR spectra showed that the relative amount of lipids in leaves was increased following exposure to both NMs. This result is in agreement with studies performed on spinach, where TiO_2-NPs also increased the level of lipids after a foliar contamination[33,35,62]. Using FTIR analysis, several studies also reported that metal-based NMs increased the relative amount of lipids in *Raphanus sativus* (Ag-NPs)[34] and in *Coriandrum sativum* (CeO_2-NPs)[33]. Lipid accumulation is one of the plant responses to various stresses such as high temperature, drought or heavy metals[63,64]. Changes in the lipid composition and/or interactions between lipids and specific membrane proteins can occur in order to reinforce the phospholipid membrane to resist the stress[65].

Differences in the FTIR spectra also occurred in the protein region. Several studies reported that NMs can impact proteins (increased or decreased content; *i.e.* proteins involved in redox regulation), depending on the exposure dose and the type of plant species[66]. In particular, FTIR analysis also demonstrated a decrease in amide (both primary and secondary) in cucumber fruits and tomato leaves after exposure to TiO_2-NPs[29,36].

Plant cell wall components were the most impacted after exposure to both NMs. It has been reviewed several times that abiotic and biotic stresses can modify content of primary and secondary cell wall components like cellulose and hemicellulose[37] which can in turn influence plant growth and biomass. Indeed, it has been shown thatcell wall stress feeds back to regulate microtubule organization, auxin transport, cellulose deposition, and future growth directionality[67]. For instance, in the case of drought stress, plants developed mechanisms leading to differential cell wall modifications allowing the reduction of the aerial parts while underground parts were increased to further investigate for residual water in the soil[39]. Here, cell walls of plants exposed to TiO_2-NPs were the most impacted and subsequently their growth was reduced up to 28% as well as their leaf area and biomass. Thess results are also in agreement with nanoecotoxicology studies which reported that Ag-NPs also affected cellulose and hemicellulose regions of FTIR spectra in radish sprouts (*Raphanus sativus*)[34]. TiO_2-NP exposure also lead to an increase in the lignin band area of the FTIR spectra of cucumber fruit[36] ; however, they decreased lignin relative content in tomato leaves but did not impact tomato fruit after exposure to TiO_2-contaminated sludge[29]. Cell wall components of rapeseed exposed to CNTs were also modified with a particular decrease in pectin relative amount[32]. It has finally been reported that metal lignin complexes may be formed which could be responsible for changes in plant chemical environment and could lead to modifications in their nutritional properties[33,36].

Cellulose and hemicellulose are located inside primary cell walls and are responsible for the cell wall rigidity[39]. Cellulose provides mechanical strength for load-bearing due to the cross-linking by

hemicelluloses[68]. Cell wall thickening represents a way for plant to resist both biotic and abiotic stress[40]. In fact, a thickening has been observed in plants as a response to mechanical intrusion of pathogens[69]. It has also been demonstrated that cellulose-deficient mutant plants are more sensitive to abiotic stress than wild type plants[37]. The increase in cellulose relative amount highlighted by FTIR could thus be a reaction of plant exposed to NMs to limit their entry through cell walls. This hypothesis is consistent with the result of the microarray profiling which demonstrated an increase in the LM19 labeling, *ie*. of lowly esterified HG, also responsible for cell wall stiffening through the formation of the so-called egg boxes with calcium ions[70].

An alternative hypothesis to the increased accumulation of this cell wall component is that it represents the main negatively charged molecule of cell walls. Indeed, HG with a low degree of methylesterification contains some amount of free carboxyl groups which can bind cations. As such, it plays a crucial role as a buffer by sequestrating positively charged molecules such as most heavy metals[40,71,72]. Using quantum dots (QD, NPs with diameter < 10 nm), some authors showed that NPs can directly interact with cell walls either through hydrogen bonds with cellulose –OH groups or via the conjugated C-C or C=C chains in lignin[73,74]. Furthermore, a recent study assessed the influence of NP surface charge on their fate in plants and demonstrated an accumulation of negatively charged QD in cell walls[75]. Here, both NMs bear negative charges when analyzed in suspension. However, so far, we have no data about their status in soil. Thanks to their large surface area, NMs exhibit high adsorption properties and could thus adsorb many molecules from the soil which in turn could influence their overall surface charge. In our experiment, the increase in the amount of LM19 epitopes could indicate a higher sequestration capability in response to the presence of NM in the medium.

Another phenomenon that can be responsible for cell wall modification is the oxidative stress caused by NMs. Indeed, all types of NMs (*e.g.* carbon-based and metal based) have been reported to generate an excess of reactive oxygen species (ROS)[76]. For instance, CNTs increased ROS content in epidermis cells of

Onobrychis arenaria as well as the activity of antioxidant enzymes such as peroxidases (POX) after 15 days of exposure in hydroponic conditions[77]. TiO_2-NPs also increased the level of catalase (CAT) and ascorbate peroxidase (APX) activities in leaves of cucumber exposed for 150 days in sandy loam soil[36]. Besides, ROS can be associated with cell wall modifications since a sudden burst of ROS can lead to catalytic oxidation of various substrates of the cell wall which results in cross-linking of cell wall components and growth arrest[78]. Class III peroxidases, also involved in the regulation of oxidative stress, can promote cell wall loosening via the hydroxylic cycle[49]. Indeed, this has been demonstrated in *A. thaliana* exposed to nZVI (nano zero valent iron) in agar medium[79]. The authors concluded that root elongation was related to the potential for nZVI to lead to H_2O_2 release causing OH radical-induced cell wall loosening in roots. This was confirmed by the degradation of pectin-polysaccharides and a decrease in cell wall thickness. The modification identified in the cell wall compounds in this work may thus also be explained by the oxidative stress caused by the NMs tested which could be independent of NM internalization.

5. Conclusion

The use of FTIR spectroscopy in this study has allowed to identify similar impacts of CNTs and TiO_2-NPs on tomato leaf cell walls despite their different physico-chemical properties. Microarray profiling confirmed FTIR results and demonstrated significant modification in HG and XG for plants exposed to TiO_2-NPs associated with a transiently reduced plant development (particularly visible after 15 days of exposure). The same trend in cell wall modification was noticed for plants exposed to CNTs, though not significantly, and with no impact on plant development. FTIR is a relatively easily accessible, fast and powerful technique for a first screening approach. Although data processing is not straightforward, we have proposed a strategy based on simple statistical analysis of the data which highlighted very slight modifications induced

by NM exposure and permitted us to focus the analysis further on the cell wall composition for a more precise description of the physiological response.

Acknowledgements

Clarisse Liné received a grant from the Région Occitanie and the Université Fédérale de Toulouse. Mansi Bakshi was supported by Toulouse Tech InterLab funding (SPECPLANP). Authors have no competing interests to declare.

Bibliography

1. Jeevanandam J, Barhoum A, Chan YS, Dufresne A, Danquah MK. Review on nanoparticles and nanostructured materials: history, sources, toxicity and regulations. *Beilstein J Nanotechnol*. 2018;9(1):1050-1074. doi:10.3762/bjnano.9.98

2. Danish Consumer Council, The Ecological council DE. Welcome to The Nanodatabase. https://nanodb.dk/en/search-database/. Published 2020. Accessed December 16, 2020.

3. García-Hevia L, Valiente R, Fernández-Luna JL, et al. Inhibition of cancer cell migration by multiwalled carbon nanotubes. *Adv Healthc Mater*. 2015;4(11):1640-1644. doi:10.1002/adhm.201500252

4. Duhan JS, Kumar R, Kumar N, Kaur P, Nehra K, Duhan S. Nanotechnology: The new perspective in precision agriculture. *Biotechnol Reports*. 2017;15:11-23. doi:10.1016/j.btre.2017.03.002

5. Dresselhaus MS, Dresselhaus G, Avouris P. *Carbon Nanotubes: Synthesis, Structure, Properties, and Applications*. Springer Science & Business Media; 2003. doi:10.1007/3-540-39947-X

6. Terrones M. Carbon nanotubes: synthesis and properties, electronic devices and other emerging applications. *Int Mater Rev*. 2004;49(6):325-377. doi:10.1179/174328004X5655

7. Gupta SM, Tripathi M. A review of TiO2 nanoparticles. *Chinese Sci Bullet*. 2011;56(16):1639-1657. doi:10.1007/s11434-011-4476-1

8. Weir A, Westerhoff P, Fabricius L, Hristovski K, von Goetz N. Titanium dioxide nanoparticles in food and personal care products. *Environ Sci Technol*. 2012;46(4):2242-2250. doi:10.1021/es204168d

9. Lu P-J, Huang S-C, Chen Y-P, Chiueh L-C, Shih DY-C. Analysis of titanium dioxide and zinc oxide nanoparticles in cosmetics. *J Food Drug Anal*. 2015;23(3):587-594. doi:10.1016/j.jfda.2015.02.009

10. Sun TY, Bornhöft NA, Hungerbühler K, Nowack B. Dynamic probabilistic modeling of environmental emissions of engineered nanomaterials. *Environ Sci Technol*. 2016;50(9):4701-4711. doi:10.1021/acs.est.5b05828

11. Liné C, Larue C, Flahaut E. Carbon nanotubes : impacts and behaviour in the terrestrial ecosystem - A review. *Carbon N Y*. 2017;123:767-785. doi:10.1016/j.carbon.2017.07.089

12. Cox A, Venkatachalam P, Sahi S, Sharma N. Silver and titanium dioxide nanoparticle toxicity in plants: A review of current research. *Plant Physiol Biochem*. 2016;107:147-163. doi:10.1016/j.plaphy.2016.05.022

13. Zheng L, Hong F, Lu S, Liu C. Effect of nano-TiO2 on strength of naturally aged seeds and growth of spinach. *Biol Trace Elem Res*. 2005;104(1):083-092. doi:10.1385/BTER:104:1:083

14. Clément L, Hurel C, Marmier N. Toxicity of TiO2 nanoparticles to cladocerans, algae, rotifers and plants - Effects of size and crystalline structure. *Chemosphere*. 2013;90(3):1083-1090. doi:10.1016/j.chemosphere.2012.09.013

15. Hatami M, Ghorbanpour M. Nano-anatase TiO2 modulates the germination behavior and seedling vigority of the five commercially important medicinal and aromatic plants. *J Biol Environ Sci*. 2014;22(8):53-59.

16. Larue C, Laurette J, Herlin-Boime N, et al. Accumulation, translocation and impact of TiO2 nanoparticles in wheat (Triticum aestivum spp.): influence of diameter and crystal phase. *Sci Total Environ*. 2012;431:197-208. doi:10.1016/j.scitotenv.2012.04.073

17. Ghosh M, Bandyopadhyay M, Mukherjee A. Genotoxicity of titanium dioxide (TiO2) nanoparticles at two trophic levels: Plant and human lymphocytes. *Chemosphere*. 2010;81(10):1253-1262. doi:10.1016/j.chemosphere.2010.09.022

18. Castiglione MR, Giorgetti L, Geri C, Cremonini R. The effects of nano-TiO2 on seed germination, development and mitosis of root tip cells of Vicia narbonensis L. and Zea mays L. *J Nanoparticle Res*. 2011;13(6):2443-2449. doi:10.1007/s11051-010-0135-8

19. Vijayaraj V, Liné C, Cadarsi S, et al. Transfer and ecotoxicity of titanium dioxide nanoparticles in the terrestrial and aquatic ecosystems : a microcosm study. *Environ Sci Technol*. 2018;52(21):12757-12764. doi:10.1021/acs.est.8b02970

20. Reddy PVL, Hernandez-Viezcas JA, Peralta-Videa JR, Gardea-Torresdey JL. Lessons learned: are engineered nanomaterials toxic to terrestrial plants? *Sci Total Environ*. 2016;568:470-479. doi:10.1016/j.scitotenv.2016.06.042

21. Ray PC, Yu H, Fu PP. Toxicity and environmental risks of nanomaterials: challenges and future needs. *J Environ Sci Health C Environ Carcinog Ecotoxicol Rev*. 2009;27(1):1-35. doi:10.1080/10590500802708267

22. Sravan Kumar S, Manoj P, Giridhar P. Fourier transform infrared spectroscopy (FTIR) analysis, chlorophyll content and antioxidant properties of native and defatted foliage of green leafy vegetables. *J Food Sci Technol*. 2015;52(12):8131-8139. doi:10.1007/s13197-015-1959-0

23. Baker MJ, Trevisan J, Bassan P, et al. Using Fourier transform IR spectroscopy to analyze biological materials. *Nat Protoc*. 2014;9(8):1771-1791. doi:10.1038/nprot.2014.110

24. Szymanska-Chargot M, Zdunek A. Use of FT-IR spectra and PCA to the bulk characterization of cell wall residues of fruits and vegetables along a Fraction Process. *Food Biophys*. 2013;8(1):29-42. doi:10.1007/s11483-012-9279-7

25. Largo-Gosens A, Hernandez-Altamirano M, Garca-a-Calvo L, Alonso-Siman A, Alvarez J, Acebes JL. Fourier transform mid infrared spectroscopy applications for monitoring the structural plasticity of

plant cell walls. *Front Plant Sci*. 2014;5:303. doi:10.3389/fpls.2014.00303

26. Chylińska M, Szymańska-Chargot M, Zdunek A. FT-IR and FT-Raman characterization of non-cellulosic polysaccharides fractions isolated from plant cell wall. *Carbohydr Polym*. 2016;154:48-54. doi:10.1016/J.CARBPOL.2016.07.121

27. Gierlinger N. New insights into plant cell walls by vibrational microspectroscopy. *Appl Spectrosc Rev*. 2018;53(7):517–551. doi:10.1080/05704928.2017.1363052

28. McCann M, Hammouri M, Wilson R, Belton P, Roberts K. Fourier transform infrared microspectroscopy is a new way to look at plant cell walls. *Plant Physiol*. 1992;100(4):1940-1947. doi:10.1104/pp.100.4.1940

29. Bakshi M, Liné C, Bedolla DE, et al. Assessing the impacts of sewage sludge amendment containing nano-TiO2 on tomato plants: A life cycle study. *J Hazard Mater*. 2019;369:191-198. doi:10.1016/J.JHAZMAT.2019.02.036

30. Dao L, Beardall J, Heraud P. Characterisation of Pb-induced changes and prediction of Pb exposure in microalgae using infrared spectroscopy. *Aquat Toxicol*. 2017;188:33-42. doi:10.1016/j.aquatox.2017.04.006

31. Thumanu K, Sompong M, Phansak P, Nontapot K, Buensanteai N. Use of infrared microspectroscopy to determine leaf biochemical composition of cassava in response to Bacillus subtilis CaSUT007. *J Plant Interact*. 2015;10(1):270-279. doi:10.1080/17429145.2015.1059957

32. Liné C, Manent F, Wolinski A, Flahaut E, Larue C. Comparative study of response of four crop species exposed to carbon nanotube contamination in soil. *Chemosphere*. 2021;274:129854. doi:10.1016/j.chemosphere.2021.129854 0045-6535

33. Morales MI, Rico CM, Angel Hernandez-Viezcas J, et al. Toxicity assessment of cerium oxide

nanoparticles in cilantro (Coriandrum sativum L.) plants grown in organic soil. *J Agric Food Chem*. 2013;61:6224−6230. doi:10.1021/jf401628v

34. Zuverza-Mena N, Armendariz R, Peralta-Videa JR, Gardea-Torresdey JL. Effects of silver nanoparticles on radish sprouts: root growth reduction and modifications in the nutritional value. *Front Plant Sci*. 2016;7:1-11. doi:10.3389/fpls.2016.00090

35. Zhao L, Peralta-Videa JR, Rico CM, et al. CeO2 and ZnO nanoparticles change the nutritional qualities of cucumber (Cucumis sativus). *J Agric Food Chem*. 2014;62(13):2752-2759. doi:10.1021/jf405476u

36. Servin AD, Morales MI, Castillo-Michel H, et al. Synchrotron verification of TiO2 accumulation in cucumber fruit: a possible pathway of TiO2 nanoparticle transfer from soil into the food chain. *Environ Sci Technol*. 2013;47(20):11592-11598. doi:10.1021/es403368j

37. Le Gall H, Philippe F, Domon J-M, Gillet F, Pelloux J, Rayon C. Cell wall metabolism in response to abiotic stress. *Plants*. 2015;4(1):112-166. doi:10.3390/plants4010112

38. Alonso-Simón A, García-Angulo P, Mélida H, Encina A, Álvarez JM, Acebes JL. The use of FTIR spectroscopy to monitor modifications in plant cell wall architecture caused by cellulose biosynthesis inhibitors. *Plant Signal Behav*. 2011;6(8):1-7. doi:10.4161/psb.6.8.15793

39. Tenhaken R. Cell wall remodeling under abiotic stress. *Front Plant Sci*. 2014;5:771. doi:10.3389/fpls.2014.00771

40. Krzesłowska M. The cell wall in plant cell response to trace metals: polysaccharide remodeling and its role in defense strategy. *Acta Physiol Plant*. 2011;33:35-51. doi:10.1007/s11738-010-0581-z

41. Gautam R, Vanga S, Ariese F, Umapathy S. Review of multidimensional data processing approaches for Raman and infrared spectroscopy. *EPJ Tech Instrum*. 2015;2(1):8. doi:10.1140/epjti/s40485-

015-0018-6

42. Flahaut E, Bacsa R, Peigney A, Laurent C. Gram-scale CCVD synthesis of double-walled carbon nanotubes. *Chem Commun (Camb)*. 2003;(12):1442-1443. doi:10.1039/B301514A

43. Soil Survey Staff ., Natural Resources Conservation Service ., U.S. Department of Agriculture . *Soil Taxonomy: A Basic System of Soil Classification for Making and Interpreting Soil Surveys*.; 1999.

44. Schneider CA, Rasband WS, Eliceiri KW. NIH image to ImageJ: 25 years of image analysis. *Nat Methods*. 2012;9(7):671-675.

45. Demšar J, Erjavec A, Hočevar T, et al. *Orange: Data Mining Toolbox in Python Tomaž Curk Matija Polajnar Laň Zagar*. Vol 14.; 2013.

46. Toplak M, Birarda G, Read S, et al. Infrared Orange: connecting hyperspectral data with machine learning. *Synchrotron Radiat News*. 2017;30:40-45.

47. Türker-Kaya S, Huck CW. A review of mid-infrared and near-infrared imaging: principles, concepts and applications in plant tissue analysis. *Molecules*. 2017;22:168. doi:10.3390/molecules22010168

48. Savassa SM, Castillo-Michel H, Pradas del Real AE, Reyes-Herrera J, Rodrigues Marquesa JP, de Carvalho HWP. Ag nanoparticles enhancing Phaseolus vulgaris seedling development: understanding nanoparticle migration and chemical transformation across the seed coat. *Environ Sci Nano*. 2021;8:493-501. doi:10.1039/d0en00959h

49. Moller I, Sørensen I, Bernal AJ, et al. High-throughput mapping of cell-wall polymers within and between plants using novel microarrays. *Plant J*. 2007;50:1118-1128. doi:10.1111/j.1365-313X.2007.03114.x

50. Fox J. *An R and S-Plus Companion to Applied Regression*. Sage Publications; 2002.

51. Lenth R V. Least-Squares Means: The *R* Package **lsmeans**. *J Stat Softw*. 2016;69(1):1-33. doi:10.18637/jss.v069.i01

52. Giraudoux P, Antonietti J-P, Beale C, Pleydell D, Treglia M. Spatial Analysis and Data Mining for Field Ecologists [R package pgirmess version 1.6.9]. *J Stat Softw*. 2018.

53. Wickham H. *Ggplot2 : Elegant Graphics for Data Analysis*. Springer; 2009.

54. Lê S, Josse J, Rennes A, Husson F. *FactoMineR: An R Package for Multivariate Analysis*. Vol 25.; 2008.

55. Sene C, McCann M, Wilson R, Grinter R. Fourier-Transform Raman and Fourier-Transform Infrared Spectroscopy (An Investigation of Five Higher Plant Cell Walls and Their Components). *Plant Phys*. 1994;106(4):1623-1631. doi:10.1104/pp.106.4.1623

56. Regvar M, Eichert D, Kaulich B, Gianoncelli A, Pongrac P, Vogel-Mikuš K. Biochemical characterization of cell types within leaves of metal-hyperaccumulating Noccaea praecox (Brassicaceae). *Plant Soil*. 2013;373(1-2):157-171. doi:10.1007/s11104-013-1768-z

57. Schulz H, Baranska M. Identification and quantification of valuable plant substances by IR and Raman spectroscopy. *Vib Spectrosc*. 2007;43(1):13-25. doi:10.1016/j.vibspec.2006.06.001

58. Tourinho PS, van Gestel CAM, Lofts S, Svendsen C, Soares AMVM, Loureiro S. Metal-based nanoparticles in soil: fate, behavior, and effects on soil invertebrates. *Environ Toxicol Chem*. 2012;31(8):1679-1692. doi:10.1002/etc.1880

59. Baalousha M, Sikder M, Prasad A, Lead J, Merrifield R, Chandler GT. The concentration-dependent behaviour of nanoparticles. *Env Chem*. 2015:1-4. doi:10.1071/EN15142

60. Lešková A, Giehl RFH, Hartmann A, Fargašová A, von Wirén N. Heavy metals induce iron deficiency responses at different hierarchic and regulatory levels. *Plant Physiol*. 2017;174:1648-1668. doi:10.1104/pp.16.01916

61. Khodakovskaya M V., Kim B-S, Kim JN, et al. Carbon nanotubes as plant growth regulators: effects on tomato growth, reproductive system, and soil microbial community. *Small*. 2013;9(1):115-123. doi:10.1002/smll.201201225

62. Rico CM, Morales MI, Barrios AC, et al. Effect of cerium oxide nanoparticles on the quality of rice (Oryza sativa L.) grains. *Environ Sci Technol*. 2013;47:5635-5642. doi:10.1021/jf404046v

63. Kuczyńska A, Cardenia V, Ogrodowicz P, Kempa M, Rodriguez-Estrada MT, Mikołajczak K. Effects of multiple abiotic stresses on lipids and sterols profile in barley leaves (Hordeum vulgare L.). *Plant Physiol Biochem*. 2019;141:215-224. doi:10.1016/j.plaphy.2019.05.033

64. Nesterov VN, Rozentsvet OA, Murzaeva S V. Changes in lipid composition in the tissues of fresh-water plant Hydrilla verticillata induced by accumulation and elimination of heavy metals. *Russ J plant Physiol*. 2009;56:85-93. doi:10.1134/S1021443709010130

65. Guo Q, Liu L, Barkla B. Membrane lipid remodeling in response to salinity. *Int J Mol Sci*. 2019;20(17):4264. doi:10.3390/ijms20174264

66. Hatami M, Kariman K, Ghorbanpour M. Engineered nanomaterial-mediated changes in the metabolism of terrestrial plants. *Sci Total Environ*. 2016;571:275-291. doi:10.1016/j.scitotenv.2016.07.184

67. Cosgrove DJ. Plant cell wall extensibility: connecting plant cell growth with cell wall structure, mechanics, and the action of wall-modifying enzymes. *J Exp Bot*. 2016;67(2):463–476. doi:10.1093/jxb/erv511

68. Sattelmacher B, Horst WJ, eds. *The Apoplast of Higher Plants: Compartment of Storage, Transport and Reactions*. Dordrecht: Springer Netherlands; 2007. doi:10.1007/978-1-4020-5843-1

69. Voigt CA. Callose-mediated resistance to pathogenic intruders in plant defense-related papillae.

Front Plant Sci. 2014;5:168. doi:10.3389/fpls.2014.00168

70. Wolf S, Mouille G, Pelloux J. Homogalacturonan methyl-esterification and plant development. *Mol Plant*. 2009;2(5):851-860. doi:10.1093/mp/ssp066

71. Schwab F, Zhai G, Kern M, Turner A, Schnoor JL, Wiesner MR. Barriers, pathways and processes for uptake, translocation and accumulation of nanomaterials in plants - Critical review. *Nanotoxicology*. 2016;10(3):257-278. doi:10.3109/17435390.2015.1048326

72. Kartel M, Kupchik L, Veisov B. Evaluation of pectin binding of heavy metal ions in aqueous solutions. *Chemosphere*. 1999;38:2591–2596.

73. Djikanović D, Kalauzi A, Jeremić M, et al. Interaction of the CdSe quantum dots with plant cell walls. *Colloids Surfaces B Biointerfaces*. 2012;91(1):41-47. doi:10.1016/j.colsurfb.2011.10.032

74. Sun H, Wang M, Lei C, Li R. Cell wall: An important medium regulating the aggregation of quantum dots in maize (Zea mays L .) seedlings. *J Hazard Mater*. 2021;403:123960. doi:10.1016/j.jhazmat.2020.123960

75. Majumdar S, Ma C, Villani M, et al. Surface coating determines the response of soybean plants to cadmium sulfide quantum dots. *NanoImpact*. 2019;14:100151. doi:10.1016/j.impact.2019.100151

76. Begum P, Fugetsu B. Phytotoxicity of multi-walled carbon nanotubes on red spinach (Amaranthus tricolor L) and the role of ascorbic acid as an antioxidant. *J Hazard Mater*. 2012;243:212-222. doi:10.1016/j.jhazmat.2012.10.025

77. Smirnova E, Gusev A, Zaytseva O, et al. Uptake and accumulation of multiwalled carbon nanotubes change the morphometric and biochemical characteristics of Onobrychis arenaria seedlings. *Front Chem Sci Eng*. 2012;6(2):132-138. doi:10.1007/s11705-012-1290-5

78. Passardi F, Penel C, Dunand C. Performing the paradoxical: how plant peroxidases modify the cell

wall. *Trends Plant Sci*. 2004;9(11):534-540. doi:10.1016/J.TPLANTS.2004.09.002

79. Kim JH, Lee Y, Kim EJ, et al. Exposure of iron nanoparticles to Arabidopsis thaliana enhances root elongation by triggering cell wall loosening. *Environ Sci Technol*. 2014;48(6):3477-3485. doi:10.1021/es4043462

Figure captions

Figure 1. Morphological responses of tomato plants: plant height (A), total leaf area (B) and total fresh biomass (C) after exposure during 15 days in soil contaminated with CNTs or TiO_2-NPs at 100 or 500 $mg.kg^{-1}$ (CNT 100, CNT 500, TiO_2 100, TiO_2 500) with standard errors (n = 5). Different letters imply statistical differences ($p<0.05$). D is the PCA using all the morphological parameters (leaf number, plant height, leaf area and biomass).

Figure 2. (A) PC-LDA analysis of the normalized FTIR spectra for tomato leaves after 15 days of exposure in soil contaminated with CNTs or TiO_2-NPs at 100 or 500 $mg.kg^{-1}$ (CNT 100, CNT 500, TiO_2 100, TiO_2 500) including also the barycenter of the ellipse for each treatment. (B) Normalized FTIR spectra for tomato leaves after 15 days of exposure in soil contaminated with CNTs or TiO_2-NPs. Peaks contributing the most to differences among groups are highlighted in yellow. Peak A = 2852-2848 cm^{-1}, lipid region. Peak B = 1550-1537 cm^{-1}, amide II region. Peak C = 1320-1312 cm^{-1}, carboxyl region. Peak D = 1160-1155 cm^{-1}, polysaccharide region (cellulose). Peak E = 1082-1070 cm^{-1}, polysaccharide region (hemicelluloses). Peak F = 1052-990 cm^{-1}, pectin and various polysaccharides region.

Figure 3. PC-LDA of the FTIR spectra (between 1800-800 and 2900-2700 cm^{-1}) acquired on individual tomato leaves after 15 days of exposure in soil containing 500 $mg.kg^{-1}$ CNTs or TiO_2-NPs (Control, CNT 500 and TiO_2 500) (A youngest leaf, B intermediate leaf, C intermediate leaf and D oldest leaf). PC-LDA were run with Orange software and drawn with RStudio (ggplot2).

649 Figure 4. Polysaccharide microarray analysis of cellulose-, hemicelluloses- and pectin-enriched fractions of
650 tomato cell wall leaves exposed for 15 days to 500 $mg.kg^{-1}$ CNT or TiO_2-NPs. The detection was performed
651 on nitrocellulose membranes which were subsequently scanned. The signals were then quantified. Results
652 are expressed in intensity in comparison to the control and standard errors are indicated (n=5). LM25 is
653 specific for XG (motifs XLLG, XXLG and XXXG), LM15 for XG (motif XXXG) and LM19 for HG.

654

655 Figure 1.

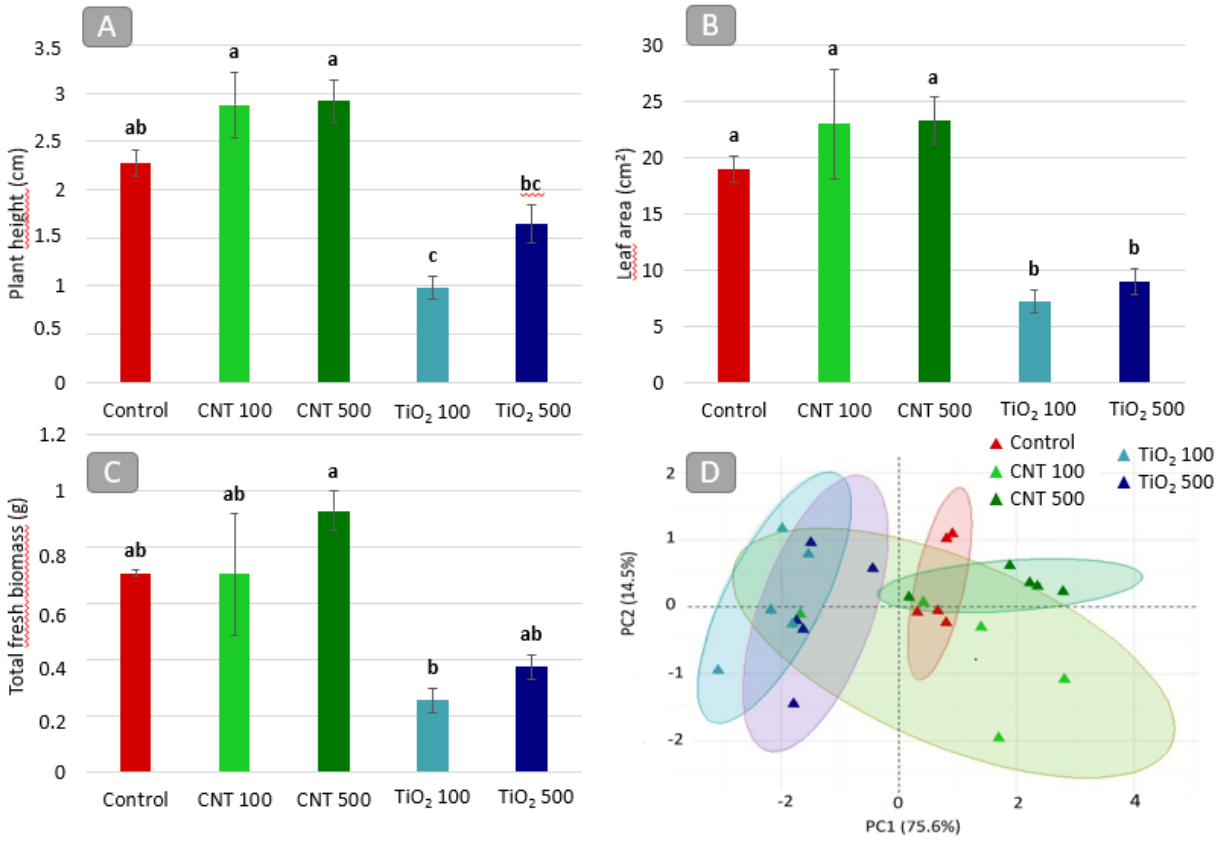

656

657

Figure 2.

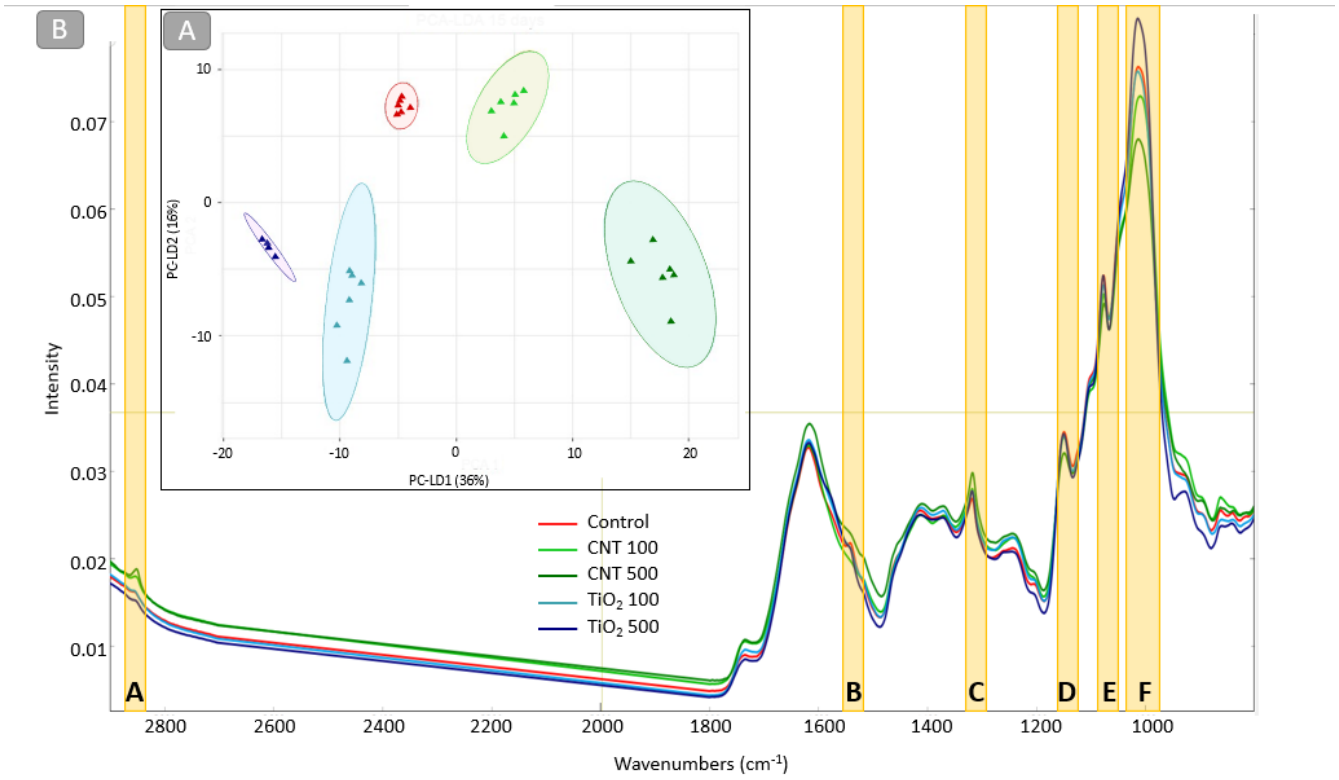
B
A
Intensity
0.07
0.06
0.05
0.04
0.03
0.02
0.01
2800
2600
2400
2200
2000
1800
1600
1400
1200
1000
Wavenumbers (cm-1)
A
B
C
D
E
F
Control
CNT 100
CNT 500
TiO2 100
TiO2 500
PC-LD2 (16%)
PC-LD1 (36%)
10
0
-10
-20
-10
0
10
20

663 Figure 3.

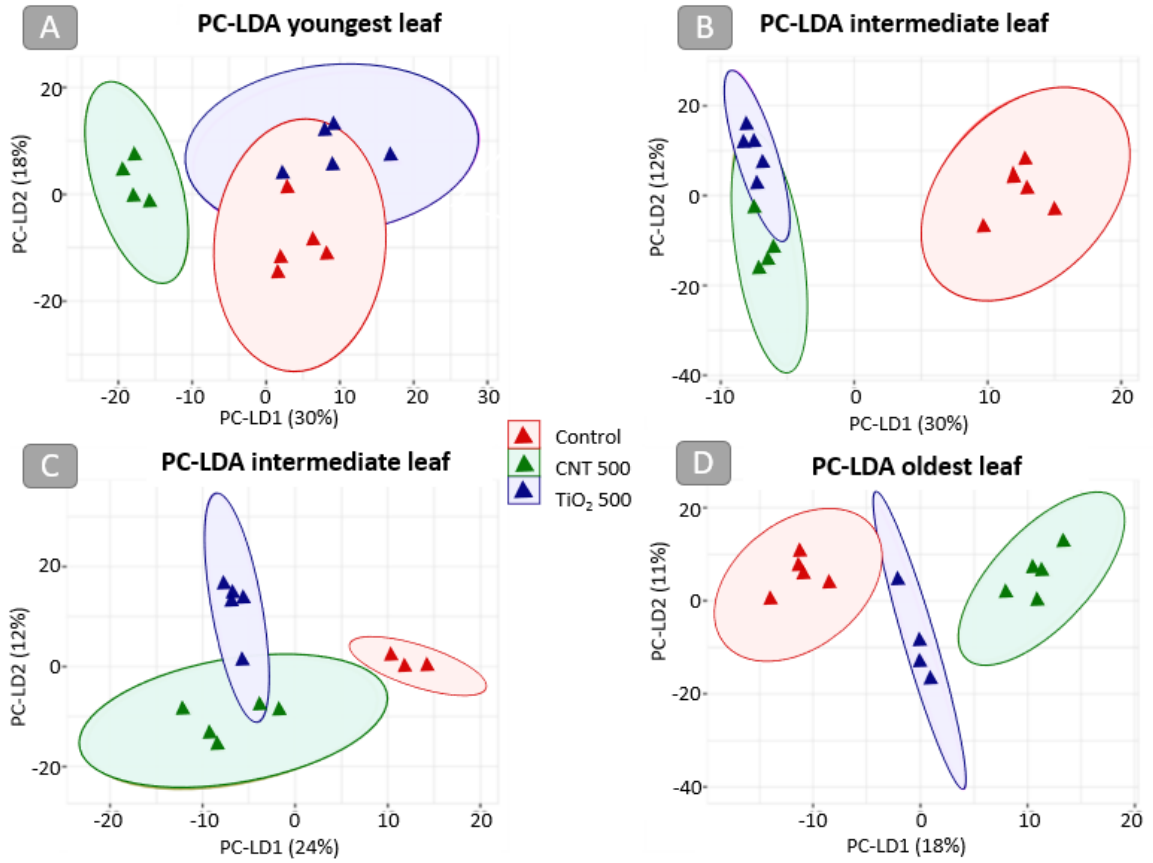

664

665

666 Figure 4.

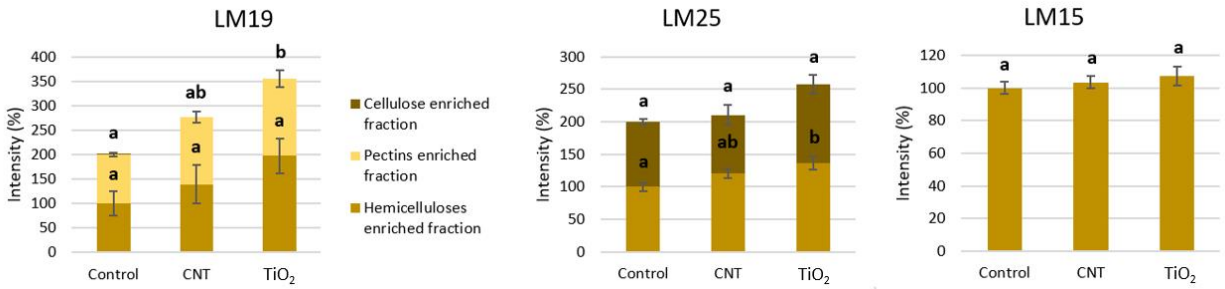

667

668

669

Table 1. Peaks contributing the most to differences among treatments extracted from the logistic regression for 15 days of exposure with the band letter corresponding to the figure 2 together with the area under the absorption peak extracted from normalized FTIR spectra the for the five different conditions (Control, CNT 100, CNT 500, TiO_2 100 and TiO_2 500). Areas are expressed in % in comparison to the control with standard errors.

Wavenumbers (cm^{-1})	**Band**	**Assignment**	**Main compounds**	**References**	**CNT 100**	**CNT 500**	**TiO_2 100**	**TiO_2 500**	**P-value**
2852 - 2848	A	CH_2 symmetric stretch	Lipids	[47,57]	+25 ± 0%	+29 ± 2%	+12 ± 2%	+6 ± 0%	<0.001
1550 - 1537	B	N-H and C=N	Amide II	[55,56]	-12 ± 1%	+1 ± 1%	-6 ± 7%	-6 ± 1%	0.041
1320 - 1312	C	C-H bend	Carboxyl groups from ligands, proteins, various polysaccharides (cellulose)	[38,47,56,57]	+5 ± 1%	+15 ± 3%	+3 ± 5%	+3 ± 1%	0.018
1160 - 1155	D	OH or C-O stretch	Various polysaccharides (mainly cellulose)	[38,47,56,57]	-1 ± 0%	-5 ± 1%	-1 ± 1%	-1 ± 1%	0.004
1082 - 1070	E	C-O ring stretch	Various polysaccharides (hemicelluloses in particular)	[38,47,56]	-5 ± 1%	-6 ± 1%	-3 ± 1%	-1 ± 0%	0.033
1052 - 990	F	O-H and C-OH stretch	Pectin, various polysaccharides	[47,56,57]	-1 ± 2%	-6 ± 1%	+2 ± 3%	+9 ± 1%	<0.001